

Hydrogen and halogen bonding patterns and π – π aromatic interactions of some 6,7-disubstituted 1,3-benzothiazoles studied by X-ray diffraction and DFT calculations

Helena Čičak^a, Marijana Đaković^b, Zlatko Mihalić^a, Gordana Pavlović^c, Livio Racané^c, Vesna Tralić-Kulenović^{c,*}

^a Laboratory of Organic Chemistry, Department of Chemistry, Faculty of Science, University of Zagreb, Horvatovac 102a, Zagreb 10000, Croatia

^b Laboratory of General and Inorganic Chemistry, Department of Chemistry, Faculty of Science, University of Zagreb, Horvatovac 102a, Zagreb 10000, Croatia

^c Department of Applied Chemistry, Faculty of Textile Technology, University of Zagreb, Prilaz baruna Filipovića 28a, Zagreb 10000, Croatia

ARTICLE INFO

Article history:

Received 23 December 2009

Received in revised form 1 April 2010

Accepted 5 April 2010

Available online 11 April 2010

Keywords:

6,7-Disubstituted 1,3-benzothiazoles

Hydrogen and Halogen bonds

π – π Interactions

X-ray structure

DFT calculations

AIM analysis

ABSTRACT

The structures of five 6,7-disubstituted 1,3-benzothiazole (1,3-benzothiazole = bta) derivatives: 6-chloro-7-nitro-bta (**3**), 6-iodo-7-nitro-bta (**5**), 6-amino-7-iodo-bta (**6**), 6-acetylamino-7-iodo-bta (**7**) and 6-amino-7-bromo-bta (**8**) are reported and investigated by X-ray crystallography and DFT calculations. The crystal structures of **3** and **5–8** are characterized by: (i) relatively weak C–H...O/N/Br and N–H...O/N/S hydrogen bonds, (ii) C–Cl...O and C–I...O/N halogen bonds and Br...Br interactions and (iii) π – π interactions.

DFT optimized structures of **3**, **5**, **6** and **8** are in a good agreement with the corresponding X-ray molecular data. Calculated structure of **7** deviates from the experimental geometry because of more favourable intermolecular hydrogen bonding in crystal phase compared to the weak intramolecular hydrogen bond in the gas phase.

The molecular electrostatic potential maps were used for predicting possible hydrogen and halogen bonding sites in structures of **3**, **5**, **6** and **8**, and AIM analysis in order to characterize the nature and strength of intermolecular interactions in all of the examined crystal structures. Experimental results agree well with AIM analysis suggesting that the detected hydrogen and halogen bonds are weak and mostly of electrostatic origin.

© 2010 Elsevier B.V. All rights reserved.

1. Introduction

Benzothiazoles are an important class of compounds currently attracting considerable interest due to their biological and biophysical properties. They exhibit antitumor [1], antimicrobial [2], and antifungal [3] activities, and can be used as β -amyloid imaging agents [4]. Variation of substituents on the benzothiazole ring affects their interactions with various potential biological targets. Functionalization by appropriate substituents is a key step in designing molecules with predefined properties such as capability of hydrogen bonding or π – π interactions. While strong hydrogen bonds have been extensively studied so far, non-conventional hydrogen bonds and halogen interactions, also occurring in these compounds, constitute rapidly growing area [5–16].

As a continuation of our recent studies on synthesis [17,18], antitumor activities [19,20], structural and computational investigations [21–23] of substituted benzothiazoles, in this paper we re-

port C–H...O/N/Br and N–H...O/N/S hydrogen bonds, C–Cl...O and C–I...O/N halogen bonds, Br...Br dihalogen interactions and π – π interactions of 6-chloro-7-nitro-bta (**3**), 6-iodo-7-nitro-bta (**5**), 6-amino-7-iodo-bta (**6**), 6-acetylamino-7-iodo-bta (**7**), and 6-amino-7-bromo-bta (**8**) studied by X-ray crystal structure analysis. DFT calculations were also performed for obtaining minimum energy and determination of possible hydrogen and halogen bonding sites of studied disubstituted benzothiazoles. Criteria based on the topological analysis of the electron density, AIM, were used in order to characterize the nature and strength of hydrogen and halogen bondings.

2. Experimental

2.1. Materials and methods

The ¹H NMR and the ¹³C NMR spectra were recorded by a Bruker Avance DPX-300 (300 MHz and 75.5 MHz, for ¹H and ¹³C, respectively). Chemical shifts are reported in ppm relative to

* Corresponding author. Tel.: +385 1 3712 566; fax: +385 1 3712 599.

E-mail address: vtralic@ttf.hr (V. Tralić-Kulenović).

TMS as an internal standard. IR spectra were recorded by Nicolet Magna 760 spectrophotometer. Elemental analyses were performed by the microanalytical laboratories of the Ruđer Bošković Institute. Melting points were determined by a Kofler block apparatus.

2.2. Preparative and crystallization procedures

6-Amino-bta (**1**) and 6-chloro-bta (**2**) were prepared as reported previously [24]. Compounds **4–8** were synthesized using analogous procedures given in the literature [25]. The novel 6-chloro-7-nitro-bta (**3**) was prepared from compound **2** by nitration reaction with a mixture of fuming nitric acid and sulphuric acid (Scheme 1).

Crystals of 6-chloro-7-nitro-bta (**3**) were prepared by recrystallization from ethanol; 6-iodo-7-nitro-bta (**5**) by recrystallization from mixture of toluene/cyclohexane (1:1); 6-amino-7-iodo-bta (**6**) by recrystallization from toluene/petrolether (5:1); 6-acetyl-amino-7-iodo-bta (**7**) by recrystallization from ethanol/dichloromethane (1:2); 6-amino-7-bromo-bta (**8**) from ethanolic solution by slow evaporation at room temperature.

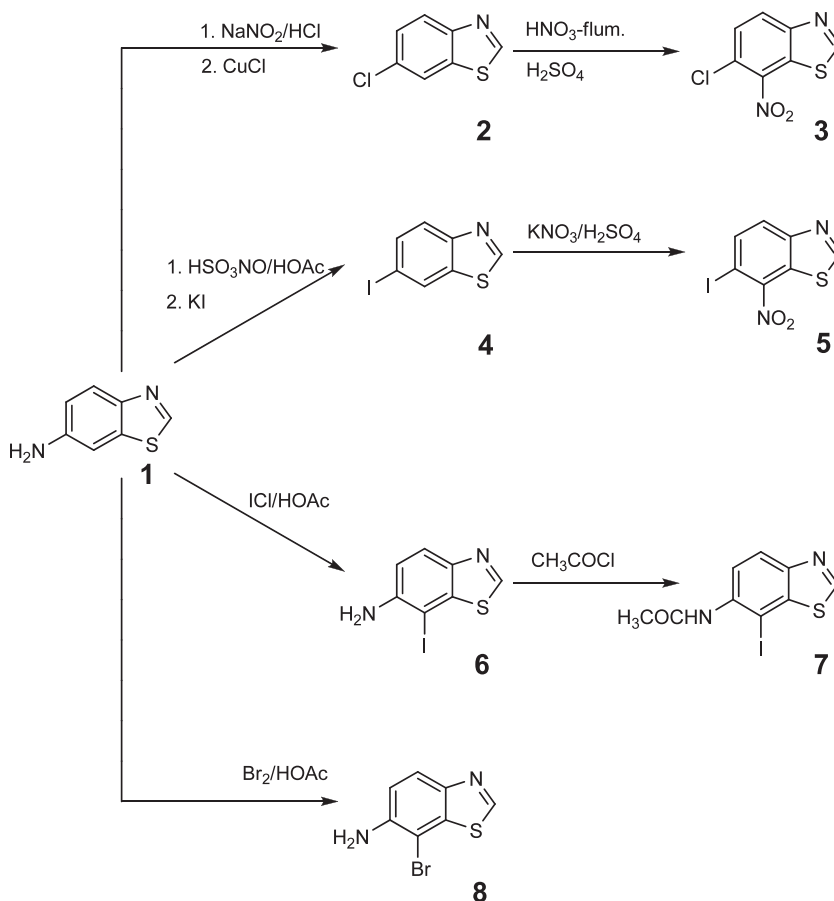
2.3. 6-Chloro-7-nitro-bta (**3**)

To a cooled mixture of 6-chloro-bta (**2**) (5.1 g, 30 mmol) in 20 mL of concd. H_2SO_4 a mixture of 10 mL HNO_3 ($d = 1.5$) and concd. H_2SO_4 was added dropwise at 5–10 °C. The reaction mixture was stirred for 3 h at room temperature, poured into cold water and basified with concd. ammonia. The resulting precipitate was filtered off, washed with water and crystallized from ethanol

giving pure product (4.4 g, 68.2%, m.p. = 140–141 °C). Elemental analysis: Calcd. (found) for $\text{C}_7\text{H}_3\text{ClN}_2\text{O}_2\text{S}$; C, 39.17 (39.03); H, 1.41 (1.50); N, 13.05 (13.07). ^1H NMR ($\text{DMSO}-d_6$, 300 MHz), δ : 9.58 (s, 1H), 8.39 (d, 1H, $J = 8.6$ Hz), 7.88 (d, 1H, $J = 8.6$ Hz). ^{13}C NMR ($\text{DMSO}-d_6$, 75 MHz), δ : 161.5, 153.7, 140.5, 132.4, 130.9, 129.5, 126.6. IR (KBr): 3087, 3063, 1592, 1512, 1333, 1304, 848, 822.

2.4. X-ray single crystal diffraction experiment

Selected crystallographic and refinement data for structures **3**, **5–8** obtained by the single crystal X-ray diffraction method are reported in Table 1. Data collections were carried out on an Oxford Diffraction four-circle kappa geometry diffractometer with Sapphire-3 CCD detector (Mo radiation with graphite monochromator) by applying the CrysAlis software system [26] at 296 K. The unit cell parameters were calculated and refined from the full data set, the Lorentz-polarization effect was corrected and the intensity data reduced by the CrysAlis RED program [26]. The diffraction data were corrected for absorption effects by the multi-scanning method. All structures were solved by direct methods and refined on F^2 by weighted full-matrix least-squares. Programs SHELXS97 and SHELXL97 [27] integrated in the WinGX software system [28] were used to solve and refine all five structures. All non-hydrogen atoms were refined anisotropically. The H atoms of amino groups in **6** and **8** were located in Fourier difference map and constrained to an ideal geometry [$\text{N}-\text{H} = 0.86 \text{ \AA}$], while in **7**, H atom attached to the amine N atom was placed in geometrically idealized position. All other hydrogen atoms were included in the refinement at calculated positions in the riding-model approxima-



Scheme 1. Synthesis of compounds **3**, **5–8**.

Table 1
General and crystal data and summary of intensity data collection and structure refinement for compounds **3**, **5**–**8**.

Compound	3	5	6	7	8
Formula	C ₇ H ₃ ClN ₂ O ₂ S	C ₇ H ₃ IN ₂ O ₂ S	C ₇ H ₃ IN ₂ S	C ₉ H ₇ IN ₂ OS	C ₇ H ₅ BrN ₂ S
M _r	214.63	306.08	276.1	318.14	229.1
Crystal system	Monoclinic	Monoclinic	Orthorhombic	Monoclinic	Orthorhombic
Colour and habit	Dark yellow, prism	Yellow, prism	Yellow–reddish, prism	Pale yellow, plate	Colourless, irregular prism
Space group	P2 ₁ /c	P2 ₁	P2 ₁ 2 ₁ 2 ₁	P2 ₁	I 4 ₁ /a
Crystal dimensions (mm ³)	0.62 × 0.34 × 0.22	0.47 × 0.39 × 0.32	0.61 × 0.54 × 0.37	0.62 × 0.44 × 0.13	0.53 × 0.49 × 0.45
Unit cell parameters:					
a (Å)	3.8851(7)	4.1437(7)	4.1698(5)	4.7726(5)	19.526(2)
b (Å)	13.737(2)	12.948(2)	13.454(1)	6.7351(6)	19.526(2)
c (Å)	15.263(3)	16.747(2)	14.9533(8)	16.2194(14)	8.1404(8)
α (°)	90	90	90	90	90
β (°)	96.16(1)	91.661(12)	90	90.973(7)	90
γ (°)	90	90	90	90	90
V (Å ³)	809.9(2)	898.1(2)	838.88(13)	521.28(8)	3103.7(5)
Z	4	4	4	2	16
D _c (g cm ⁻³)	1.76	2.264	2.186	2.027	1.961
μ (mm ⁻¹)	0.69	3.763	3.998	3.239	5.493
F(0 0 0)	432	576	520	304	1792
2θ range for data collection (°)	8, 54	8, 54	8, 54	8, 54	8, 54
h, k, l range	−4:4, −17:17, −19:19	−5:5, −16:16, −21:20	−5:5, −17:17, −19:19	−6:6, −8:8, −20:20	−24:24, −24:24, −10:10
Scan type	ω	ω	ω	ω and φ	ω
No. measured reflections	9229	11,114	7673	6459	17,738
No. independent reflections (R _{int})	1751 (0.117)	3852 (0.067)	1791 (0.051)	2165(0.083)	1695(0.154)
No. refined parameters	118	235	101	128	101
No. observed reflections, I ≥ 2σ(I)	1610	3601	1787	2143	1677
g ₁ , g ₂ in w ^a	0.0652, 0.6021	0.0718, 1.1408	0.0535, 0.9038	0.1072, 0.0258	0.0325, 10.9442
R ^b , wR ^c [I ≥ 2σ(I)]	0.0486, 0.1230	0.0450, 0.1191	0.0297, 0.0831	0.0511, 0.1321	0.0468, 0.1104
R, wR [all data]	0.0587, 0.1271	0.0476, 0.1230	0.0297, 0.0832	0.0514, 0.1329	0.0480, 0.1109
Goodness of fit on F ² , S ^d	1.045	1.062	1.085	1.105	1.151
Extinction coefficient	none	none	0.006(1)	none	0.0014(2)
Max., min. electron density (e Å ⁻³) ^e	0.681, −0.850	0.873, −1.219	0.754, −1.109	1.443, −1.577	0.830, −0.508
Maximum Δ/σ	0.000	0.000	0.001	0.000	0.000

Data in common: diffractometer used for data collection: CrysAlis, Version 171.23 (Oxford Diffraction, 2004) with λ(Mo Kα) = 0.71073 Å at 296 K.

^a $w = 1 / [\sigma^2(F_o^2) + [g_1P + g_2P]]$ where $P = (F_o^2 + 2F_c^2) / 3$.

^b $R = \sum |F_o - F_c| / \sum |F_o|$.

^c $wR = [\sum (F_o^2 - F_c^2)^2 / \sum w(F_o^2)]^{1/2}$.

^d $S = \sum [w(F_o^2 - F_c^2)^2 / (N_{obs} - N_{param})]^{1/2} .2$

^e In structures **5**, **7** and **8** the max. electron density in the last difference Fourier map is near halogen atoms, in **3** near O2 and in **6** near C5 and I1 atoms 0.75 and 0.72 e Å⁻³, respectively).

tion, with Csp²–H and Csp³–H distances of 0.93 and 0.96 Å, respectively. The U_{iso}(H) amounts 1.2 of U_{eq}(C) or U_{eq}(N) in all cases, except for hydrogen of methyl group [U_{iso}(H) = 1.5 of U_{eq}(C)]. The absolute structure of **5**, **6** and **7** has been established by the Flack's parameters values, which are all zero within the standard uncertainties.

The molecular geometry calculations and drawings were performed by PLATON [29], ORTEP-3 for Windows [30] and Mercury [31]. The thermal ellipsoids are drawn at the 50% probability level at 293 K. The Ortep drawings are shown on Figs. 1A–5A.

2.5. Computational methods

Density functional theory (DFT) calculations were carried out with the Gaussian 03 program [32]. B3LYP hybrid method, which uses Becke's three-parameter exchange functional and gradient-corrected correlation functional of Lee, Yang and Parr [33], was employed to predict the minimum energy molecular geometries of five 6,7-disubstituted btas **3**, **5**–**8**. The geometries were fully optimized in the gas phase with tight convergence criteria using Pople valence triple zeta 6-311+G(d,p) basis set for all the atoms except iodine, for which it does not exist. Therefore 6-311G(d,p) basis set was used for iodine [34]. The harmonic vibrational analysis was performed at the same level of theory in order to verify that all of the vibrational frequencies were real, confirming the structure as minimum.

Comparison of the computational results and the experimentally determined structures was performed with Maestro 9.0 pro-

gram [35] by aligning equivalent atoms in superimposed structures and calculating the root-mean-square deviation (RMSD) and the maximum difference between superimposed atoms.

Values of molecular electrostatic potential (MEP) were calculated at isodensity surface of contour value 0.0007 a.u. of previously optimized structures in order to find regions of positive and negative MEP and hence to predict possible sites capable of electrostatic interactions. Negative MEP (electron-rich) regions are coloured red, positive MEP (electron-poor) regions are blue, and zero MEP regions are green. Value of the MEP is given by the intensity of colour. The MEP maps were visualized by GaussView program [36]. The hydrogen and halogen bonding characteristics of the studied crystal structures have been investigated by the Badger's theory of "Atoms in Molecules" (AIM) [37–39]. The wave functions were obtained by single point calculations at the abovementioned level of theory for neighbouring molecules containing short contact(s) at the geometry taken from the crystal structure. The bond critical points (BCPs) were found and analyzed in terms of the electron density, its Laplacian and the electron energy density. The topological analysis was performed with the help of AIM2000 [40] and AIMAll [41] programs.

3. Results and discussion

3.1. Crystal structures description

A survey of the Cambridge Structural Data base (CSD) conducted on version 5.30 (including update 4, September 2009)

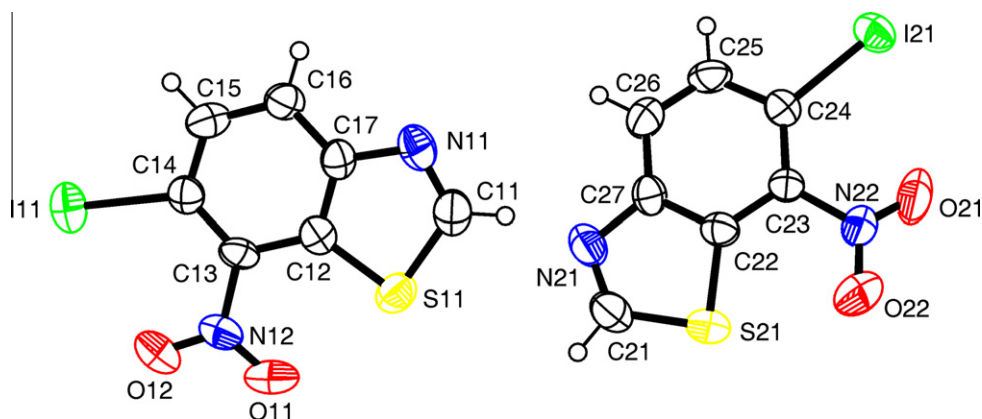


Fig. 2A. The ORTEP drawing of 6-iodo-7-nitro-bta (**5**) with atom numbering scheme of the asymmetric unit.

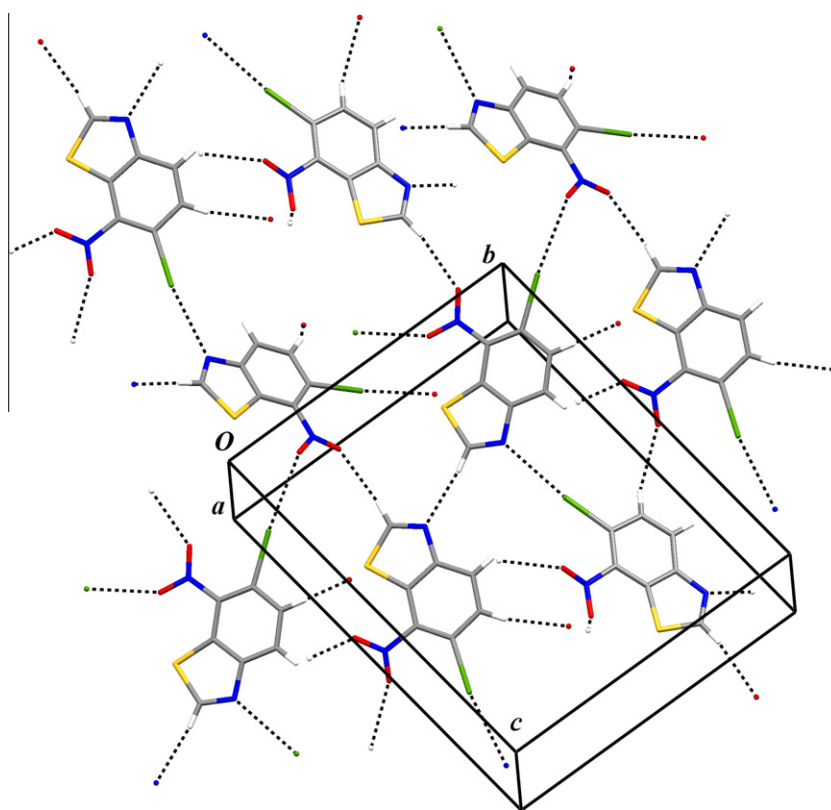


Fig. 2B. Perspective view of crystal packing of **5**. Hydrogen and halogen bonds are shown by dashed lines.

[1.56 Å] bond [44], while the C–N endocyclic bond within the thiazole fragment is dominantly double in character C1–N1 1.285(4) Å in **3**, 1.30(1) and 1.26(1) Å in **5**, 1.288(7) Å in **6**, 1.247(9) Å in **7** and 1.277(6) Å in **8** [45] (Table 2). The bond angles around the S atom are within the range found in the five-membered thiazole rings of reported mono- and disubstituted bta and its derivatives [18,21,25]. The differences in the C–C bonds within benzene ring are common for such fused rings.

The crystal structures **3** and **5–8** are determined by three factors: (i) relatively weak C–H...O/N/Br and N–H...O/N/S hydrogen bonds, (ii) C–Cl...O and C–I...O/N halogen bonds and Br...Br interactions, and (iii) π – π interactions [46–49]. The pertinent structural parameters of hydrogen- and halogen-bonded contacts are collected in Table 3, while the details of π – π geometries are given in Table 4.

In the crystal structure of **3** the hydrogen bonding intermolecular interactions are not well pronounced, only some very weak ones, far above the 3.5 Å limit are observed. The crystal packing is mainly determined by C–Cl...O halogen–nitro bonds. Two such bonds are formed between two neighbouring molecules creating double halogen bonded centrosymmetrical dimers [C11...O2 = 3.104(3) Å] (Fig. 1B). The chlorine–oxygen contact is well below the sum of van der Waals radii (3.3 Å). The observed interaction is in accordance with the results given by Allen et al. [50]. They studied geometrical preferences of halogen...O(nitro) supramolecular synthons and found that for chlorine there is a strong tendency to form interactions with only one oxygen atom of nitro group, rather than bifurcated contacts with both oxygens. The latter arrangement is typical for iodine and to some extent for bromine, e.g. the tendency to form such bifurcated motifs increases

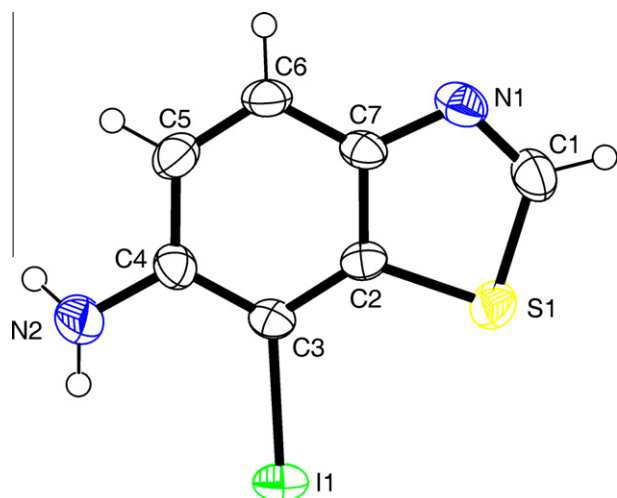


Fig. 3A. The ORTEP drawing of 6-amino-7-iodo-bta (**6**) with atom numbering scheme of the asymmetric unit.

in the order $\text{Cl} < \text{Br} < \text{I}$. Furthermore, the molecules are packed in such way that bta planes of supramolecular dimers are in stacks along $[1\ 0\ 0]$ direction with the distance between the centroids of their thiazole and benzothiazole rings of $3.723(2)\ \text{\AA}$.

Distinctly to all other described compounds, the crystal structure of compound **5** contains two symmetrically independent molecules. Consequently, different kinds of intermolecular interactions are observed involving these two molecules (Fig. 2B). The carbon atoms of the thiazole rings, C11 and C21, as well as the carbon atoms of the benzene rings, C15 and C25, of both molecules all act as hydrogen bond donors for weak $\text{C-H}\cdots\text{N}$ and $\text{C-H}\cdots\text{O}$ hydrogen bondings with the thiazole nitrogen and nitro oxygen atoms forming three-dimensional supramolecular structure. In

addition, both iodine atoms, I11 and I21, are found to be involved into halogen bonding with oxygen atom of nitro group, O11 [$\text{I11}\cdots\text{O11} = 3.11(1)\ \text{\AA}$], and the thiazole ring nitrogen atom, N11 [$\text{I21}\cdots\text{N11} = 3.044(8)\ \text{\AA}$], both belonging to the first molecule. The substitution of chlorine atom in **3** with iodine atom in **5** did not give the typical bifurcated contacts of iodine atom with both oxygen atoms of nitro group [50]. Furthermore, the molecules are additionally stabilized by the π - π stacking interactions established between the thiazole and benzene rings in $[1\ 0\ 0]$ direction.

The hydrogen bonding interactions are in the crystal structure of compound **6** not well pronounced. The supramolecular structure is dominated by weak $\text{N-H}\cdots\text{S}$ and $\text{C-H}\cdots\text{N}$ hydrogen bonds (Fig. 3B). The former interaction, found between the amine group hydrogen atoms and the thiazole sulphur atom, forms the endless $\text{C}(6)$ zig-zag chains in $[0\ 1\ 0]$ direction [51,52], while the latter one, observed between the thiazole carbon and nitrogen atoms of two

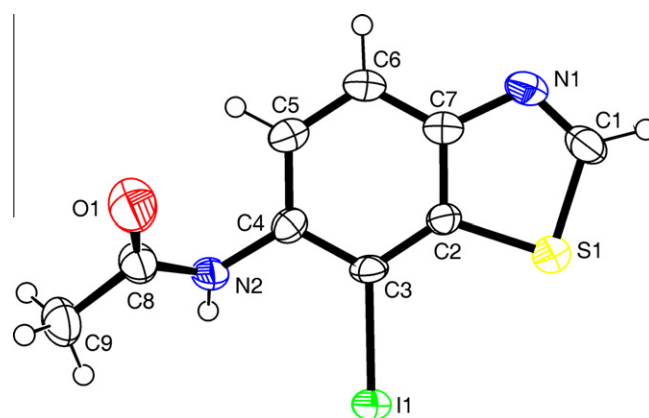


Fig. 4A. The ORTEP drawing of 6-acetylamino-7-iodo-bta (**7**) with atom numbering scheme of the asymmetric unit.

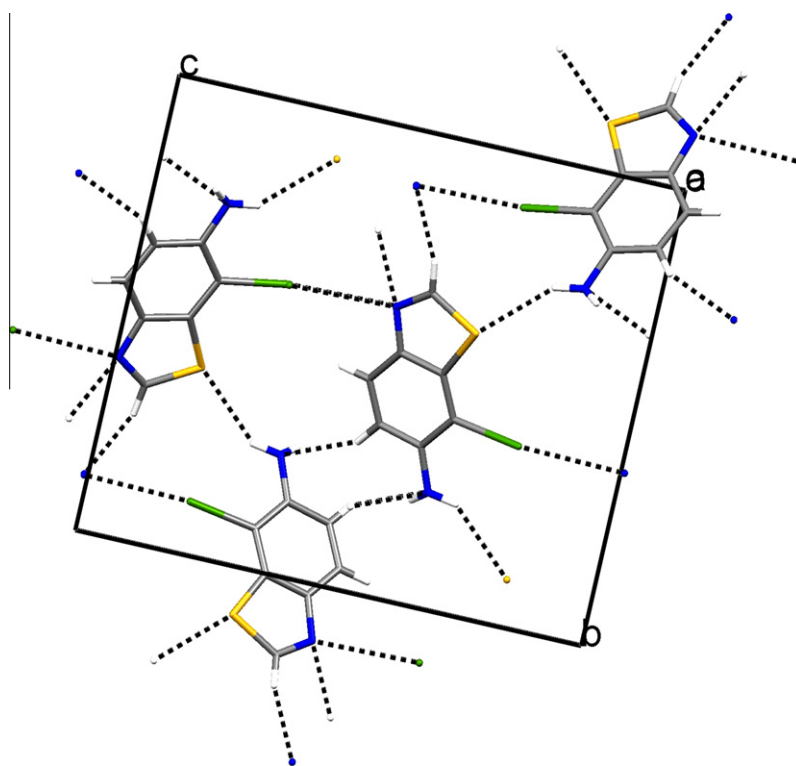


Fig. 3B. Crystal packing of **6** shown down the a axis. Hydrogen and halogen bonds are presented by dashed lines.

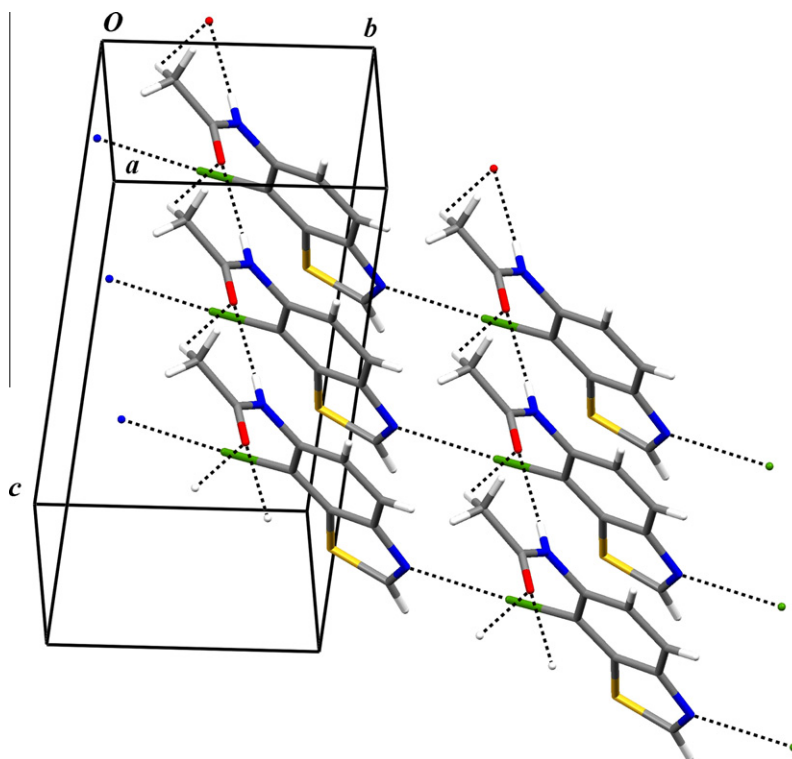


Fig. 4B. Packing diagram of **7**, showing N—H...O, C—H...O hydrogen and C—I...N halogen interactions as dashed lines. The hydrogen bonds forms C(4) $[R_2^1(6)]$ chains in [1 0 0] direction.

neighbouring molecules, forms C(3) zig-zag chains in [1 0 0] direction. Interestingly, the thiazole nitrogen atom additionally acts as acceptor for one more interaction, this time it accepts iodine as well, forming short I...N contact of 3.206(5) Å, well below the sum of van der Waals radii (3.5 Å). Moreover, there exist one more weak hydrogen bonding interaction in [1 0 0] direction involving donating benzene ring carbon atom C5 and accepting amine nitrogen atom N2. This interaction forms helical C(4) chains. Furthermore, the molecules are also in stacks in [1 0 0] direction with the distance between the centroids of their thiazole and benzene rings of 3.819(3) Å, resulting in similar stacking interactions as observed in structures **3** and **5**.

The supramolecular structure of compound **7** contains stronger N—H...O hydrogen bonds utilizing the acetylamino N and O atom of adjacent molecules forming amide C(4) chains (Fig. 4B). Additionally, the methyl carbon atom C9 is involved into weak hydrogen bonding interaction with the same accepting atom O1. The two described interactions form the chains of molecules in [1 0 0] direction that could be described by graph-set notation of C(4) $[R_2^1(6)]$. These chains are further organized into two-dimen-

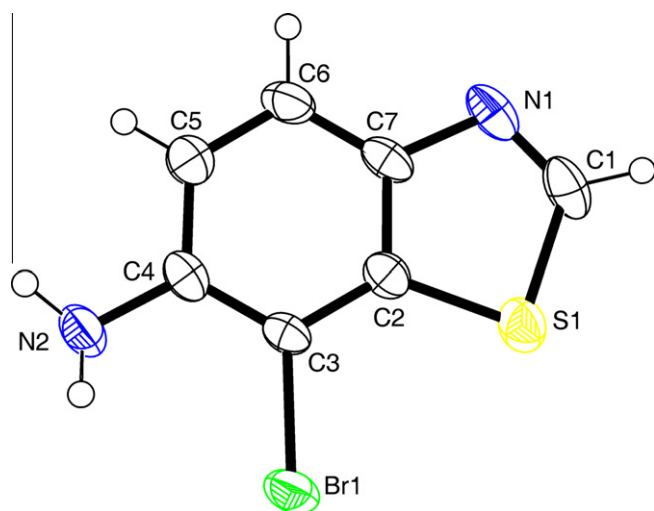


Fig. 5A. The ORTEP drawing of 6-amino-7-bromo-bta (**8**) with atom numbering scheme of the asymmetric unit.

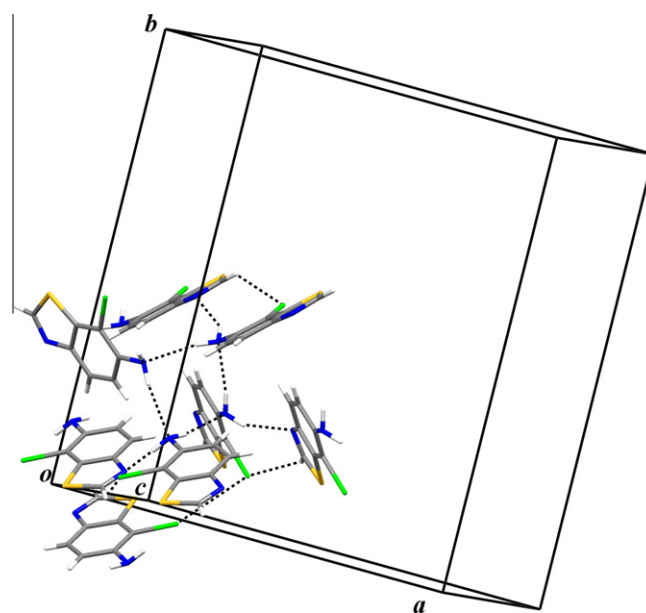
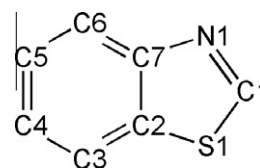


Fig. 5B. A partial packing diagram of **8**, representing the $R_4^1(8)$ motif formed between the amino groups of four neighbouring molecules. Hydrogen bonds are shown by black dashed lines.

sional supramolecular sheets in (1 0 0) planes by C3–I1···N1 halogen bonds [$I \cdots N = 3.027(6) \text{ \AA}$]. The crystal structure of **7** is the only one of the described in this paper where π – π interactions are not observed.

The crystal structure of **8**, presented on Fig. 5B, is dominated by two moderately weak N–H···N hydrogen bonds. The hydrogen bonding between two amino groups of four neighbouring molecules forms interesting hydrogen bonding ring structure described by $R_4^4(8)$ graph-set notation. While one hydrogen atom of amino group is accepted by amino group nitrogen atom, N2, the other one is accepted by the thiazole nitrogen atom, N1. The later interaction form discrete D(3) graph-set motifs. These two interactions form three-dimensional supramolecular structure. Interestingly, the bromine atom is not involved into halogen bonding with the thiazole nitrogen atom as it is already involved into significantly stronger N–H···N hydrogen bonding. Consequently, the bromine acts as the hydrogen bonding acceptor in weak C1–H1···Br1 hydrogen bond. Additionally, the short Br···Br contact of

$3.6683(3) \text{ \AA}$ are found in **8** that are comparable with the sum of van der Waals radii (3.7 \AA [53]; 3.9 \AA [54]). The off-set stacking interactions are found in the structure of compound **8** as well, but this time between the thiazole and benzene rings with the distance between centroids of $3.894(2) \text{ \AA}$.



Scheme 2. The bta moiety without any substituents and hydrogen atoms.

Table 3
Hydrogen and halogen bonds geometry (\AA , $^\circ$) for compounds **3**, **5**–**8**.

D–H/X···A	D–H/X	H/X···A	D···A	\angle D–H/X···A	Symmetry code
Compound 3					
C4–Cl1···O2	1.722(4)	3.104(3)	4.821(4)	174.2(1)	$-x, 1-y, -z$
Compound 5					
C11–H11···N21	0.93	2.52	3.43(1)	165	x, y, z
C21–H21···O12	0.93	2.46	3.39(2)	171	$-3-x, -1/2+y, -2-z$
C15–H15···O21	0.93	2.66	3.47(1)	147.1	$-2+x, 1+y, z$
C25–H25···O21	0.93	2.54	3.42(2)	157	$-x, 1/2+y, -1-z$
C14–H11···O11	2.110(8)	3.11(1)	5.21(1)	173.7(3)	$-4-x, 1/2+y, -2-z$
C24–H21···N11	2.088(7)	3.044(8)	5.12(1)	170.7(3)	$-1-x, -1/2+y, -1-z$
Compound 6					
N2–H22 N···S1	0.86	2.80	3.501(5)	140	$2-x, 1/2+y, -3/2-z,$
C1–H1···N1	0.93	2.53	3.432(6)	163	$-1/2+x, -3/2-y, -1-z$
C3–H1···N1	2.100(4)	3.206(5)	5.289(6)	170.8(1)	$3/2-x, -1-y, -1/2+z$
Compound 7					
N2–H2···O1	0.86	2.08	2.917(6)	164.0	$-1+x, y, z$
C9–H9B···O1	0.96	2.54	3.219(9)	127.8	$-1+x, y, z$
C3–H1···N1	2.079(6)	3.027(6)	5.100(8)	174.9(2)	$-1+x, -1+y, z$
Compound 8					
N2–H12 N···N1	0.88	2.510	3.285(5)	148	$x, y, 1+z$
N2–H22 N···N2	0.91	2.420	3.324(5)	170	$-1/4-y, -1/4+x, 7/4-z$
C1–H1···Br1	0.93	2.937	3.641(4)	124	$x, y, z-1$

Table 4
Geometrical parameters of π – π interactions (\AA , $^\circ$) for compounds **3**, **5**–**8**.

Interaction ^a	Cg–Cg distance	Cg···P1 ^b	Cg···P2 ^c	α^d	β^e	$(\text{Cg–Cg}) \times \sin \beta^f$
3						
Cg1–Cg2 ⁱ	3.7231(15)	3.4915(10)	3.4964(9)	0.47(11)	20.10	1.279
5						
Cg1–Cg2 ⁱ	3.895(5)	3.697(4)	3.681(3)	0.7(4)	19.08	1.273
6						
Cg1–Cg2 ⁱ	3.819(3)	3.562(2)	3.556(2)	0.3(2)	21.42	1.395
8						
Cg1–Cg2 ⁱⁱ	3.894(2)	3.4838(15)	3.4838(15)	0	26.53	1.739

^a Ring Cg1 is defined by the atoms S1, C1, N1, C7, C2 (thiazole ring atoms) in **3**, **6** and **8** and by the atoms C22, C23, C24, C25, C26, C27 (phenyl ring atoms) in **5**. Cg2 is defined by the atoms S1, C1, N1, C7, C6, C5, C4, C3, C2 (benzothiazole ring atoms) in **3**, C2, C3, C4, C5, C6, C7 (phenyl ring atoms) in **6** and **8** and by the atoms S21, C21, N21, C27, C22 (thiazole ring atoms) in **5**.

^b Cg···P1 is the perpendicular distance of corresponding centroid to a plane. Planes P1 or P2 are defined by the atoms, which define the corresponding centroids.

^c Cg···P2 is the perpendicular distance of corresponding centroid to a plane. Planes P1 or P2 are defined by the atoms, which define the corresponding centroids.

^d Dihedral angle between P1 and P2.

^e Angle between Cg–Cg distance and Cg···P1.

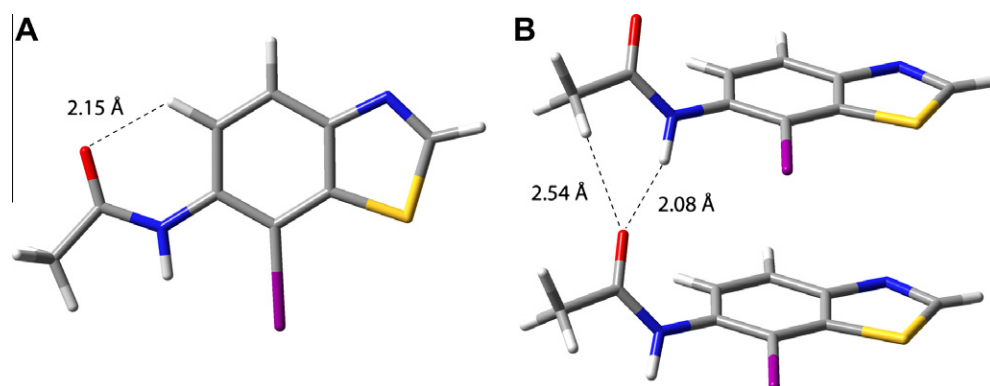
^f Offset.

ⁱ $-1+x, y, z$.

ⁱⁱ $-x, -y, 1-z$.

Table 5The root-mean-square deviation (RMSD) and the maximum difference (d_{\max}) between superimposed atom positions of the X-ray and calculated molecular structures of **3**, **5**–**8**.

Structure	bta ^a			all ^b		
	RMSD (Å)	d_{\max} (Å)	Atom pair ^c	RMSD (Å)	d_{\max} (Å)	Atom pair ^c
3	0.016	0.027	S1–S1	0.087	0.222	O2–O2
5–1	0.024	0.037	S11–S1	0.109	0.287	O12–O2
5–2	0.029	0.043	C23–C3	0.104	0.252	O21–O1
6	0.022	0.033	C1–C1	0.039	0.083	I1–I1
7	0.035	0.060	S1–S1	0.425	1.149	O1–O1
8	0.021	0.035	C1–C1	0.051	0.130	N2–N2

^a Only bta moiety without any substituents and hydrogens.^b All non-hydrogen atoms.^c Maximum difference superimposed exp-calc atom pair.**Fig. 6.** Intramolecular interaction in calculated structure (A) and intermolecular interactions in X-ray structure (B) of compound **7**.

3.2. Computational results

3.2.1. Molecular structures

In order to verify the accuracy of used theoretical model all of the investigated molecules were fully optimized in the gas phase and obtained geometries compared with the experimental ones. RMSD values between equivalent atom pairs were calculated for: (1) bta moiety without any substituents and hydrogens (Scheme 2), and (2) all non-hydrogen atoms (Table 5). First RMSD values are all smaller than 0.04 Å indicating good matching of bta moieties. Maximum differences (d_{\max}) and corresponding equivalent atoms are given in the next two columns. The d_{\max} values belong to S1_{exp} and S1_{calc} or C1_{exp} and C1_{calc} atom pairs of thiazole part, except C23_{exp} and C3_{calc} pair in **5–2**. Second RMSD values go up to 0.11 Å for structures **3**, **5**, **6** and **8**, while for **7** it is much larger (0.425 Å). The d_{\max} values belong to one oxygen atom of nitro group in **3** and **5**, iodine atom in **6**, oxygen atom of acetylamino group in **7** and nitrogen atom of amino group in **8**. As a result of superposition, it can be concluded that four calculated structures of **3**, **5**, **6** and **8** are in good agreement with X-ray molecular structures, while the calculated structure of **7** is not.

The calculated structures of **3**, **5**, **6** and **8** have no symmetry, while that of **7** has plane of symmetry (C_s point group). In optimized structure of **7**, there is an intramolecular hydrogen bond between C5–H5...O1 of 2.15 Å forming six-membered ring (Fig. 6A). In the X-ray crystal structure of **7** two intermolecular hydrogen bonds N2–H2...O1 (2.08 Å) and C9–H9B...O1 (2.54 Å) are formed between adjacent molecules also making six-membered $R_2^1(6)$ ring (Fig. 6B). The reason for that difference is that two hydrogen bonds observed in solid state are stronger than intermolecular hydrogen bond obtained by calculation on single molecule in the gas phase.

Except of different environment in theoretical calculation and X-ray diffraction experiment, it is also known that geometry can

slightly depend on the method and the basis set used. Besides good matching of calculated structures of **3**, **5**, **6** and **8** with experimental ones, it is also generally considered that used calculation model gives geometries which can be reliably used in other molecular properties calculations.

3.2.2. Molecular electrostatic potential maps

The molecular electrostatic potential has been successfully used for predicting sites participating in electrostatic interactions and hydrogen bondings [55–57].

Because of the geometric and electronic similarity of molecules **3** and **5**, as well as **6** and **8**, there are two types of the electrostatic potential maps, type I and type II, respectively (Fig. 7A). They show positive MEP regions (blue¹ colour) associated with the acidic H atoms bonded to C1 in thiazole ring and C5 and C6 in benzene ring in all of the studied compounds, as well as H atoms of NH₂ group in molecules **6** and **8**. Negative MEP regions (red colour) are associated with O1 and O2 atoms in NO₂ group in **3** and **5**, N2 atom of NH₂ group in **6** and **8** and with N1 and S1 atoms in thiazole ring and halogen atoms in all studied compounds. All these regions, or, to be more accurate, atoms associated with them, are capable of forming hydrogen bonds either as hydrogen donors, D–H (blue regions), or hydrogen acceptors, A (red regions). They are given in Table 6. N2 atoms of NO₂ group in molecules **3** and **5** are also positive.

Halogen atom (X) needs special attention because it can act as: (1) hydrogen (proton) acceptor forming D–H...X hydrogen bond, which has already been mentioned, (2) electron acceptor forming short contact with atom containing lone pair (Lewis base), X...Y (Y = nitrogen, oxygen, etc.) or (3) participant of the halogen...hal-

¹ For interpretation of color in Figs. 1–8, the reader is referred to the web version of this article.

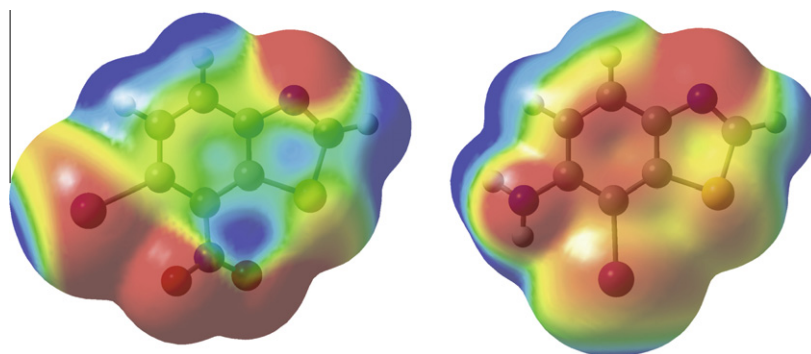


Fig. 7A. Molecular electrostatic potential maps (isovalue = 0.0007) of 6,7-disubstituted-btas **3** and **5** (type **I**, MEP range = $-0.005/+0.025$ kJ/e) and **6** and **8** (type **II**, MEP range = $-0.016/+0.025$ kJ/e).

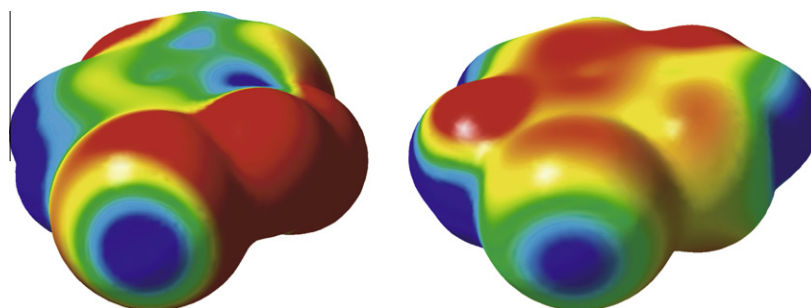


Fig. 7B. Molecular electrostatic potential maps (Isovalue = 0.0007) of 6,7-disubstituted-btas **3** and **5** (type **I**, MEP range = $-0.005/+0.025$ kJ/e) and **6** and **8** (type **II**, MEP range = $-0.016/+0.025$ kJ/e) – view along the X–C bond axis.

Table 6

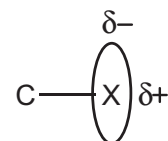
Molecular sites capable for hydrogen bonding (D–H···A) obtained by molecular electrostatic potential maps for structures of **3**, **5**, **6** and **8** (isovalue is 0.0007 a.u., MEP range in **I** is $-0.005/+0.025$ kJ/e, in **II** is $-0.016/+0.025$ kJ/e).

	3 and 5 (I)	6 and 8 (II)
<i>D–H</i> (blue)		
N2–H12 N	–	+
N2–H22 N	–	+
C1–H1	+	+
C5–H5	+	+
C6–H6	+	+
<i>A</i> (red)		
O1	+	–
O2	+	–
N1	+	+
S1	+	+
X1*	+	+
N2 (NH ₂ group)	–	+

* X1 is Cl1 in **3**, I1 in **5** and **6** and Br1 in **8**.

ogen interaction, X···X'. The essentially electrostatic X···Y or X···X' interactions (types 2 and 3) have been called halogen bonds [15]. Theoretical and experimental analyses have shown that the electron density around a bonded halogen atom is not spherically but anisotropically distributed: negative charge is concentrated in the equatorial area (*i.e.*, perpendicular to the C–X axis) and positive charge along the C–X bond, which is called σ -hole (Scheme 3). This effect, known as polar flattening, is strongly enhanced by the presence of electron withdrawing groups (e.g. nitro in *ortho* position in **3** and **5**) and also increasing in the order Cl < Br < I.

From the electrostatic potential maps (Fig. 7A and 7B) it can be seen that both studied structure types, **I** and **II**, are capable of forming halogen interactions, because blue “ σ -hole” regions and red equatorial areas exist. However, the intensities of the colours



Scheme 3. Anisotropically distributed electron density around a bonded halogen atom.

slightly vary depending on the halogen and abovementioned effects. As a consequence of multidirectional character of halogen interactions, there is the possibility of more than one interaction of single halogen atom, which can be seen in crystal structure **8** (X = Br).

3.2.3. AIM analysis

Table 7 tabulates the topological properties (electron density (ρ_b), Laplacian of electron density ($\nabla^2\rho_b$), kinetic electron energy density (G_b), potential electron energy density (V_b), total electron energy density ($H_b = V_b + G_b$) and $|V_b|/G_b$ ratio [37–39]) of the BCPs for the molecules examined in this work. Prior to discussion of the results, it is important to recall that the sign and magnitude of $\nabla^2\rho_b$ value determines a nature and strength of the interaction. When $\nabla^2\rho_b < 0$ and is large in magnitude, the electron density is also large and locally concentrated in the internuclear region. Such an interaction is shared, as is found for strong covalent or polar bond. When $\nabla^2\rho_b > 0$ and is low in magnitude, the electron density is locally depleted and interaction is closed-shell, as in ionic, hydrogen or halogen bonds and van der Waals interactions. Hence, the electron densities and their Laplacians can be used as indicators of the strengths of hydrogen and halogen bonding interactions. In addition, the sign of the total electronic energy density (H_b) is a more

Table 7
Topological parameters at H/X...A BCPs of compounds **3**, **5**–**8**.^a

D–H/X...A H/X...A	ρ_b	$\nabla^2\rho_b$	G_b	V_b	H_b	$ V_b /G_b$
Compound 3						
C4–C11...O2	0.0063	0.0300	0.0060	–0.0045	0.0015	0.7529
C4–C11...Cl1 ^b	0.0039	0.0153	0.0028	–0.0018	0.0010	0.6363
Compound 5						
C11–H11...N21	0.0125	0.0372	0.0077	–0.0061	0.0016	0.7899
C21–H21...O12	0.0104	0.0378	0.0078	–0.0061	0.0017	0.7875
C15–H15...O21	0.0077	0.0245	0.0053	–0.0045	0.0008	0.8451
C25–H25...O21	0.0084	0.0307	0.0064	–0.0050	0.0013	0.7925
C16–H16...I21 ^b	0.0054	0.0153 ^c	0.0031	–0.0024	0.0007	0.7699
C26–H26...I11 ^b	0.0028	0.0082 ^c	0.0016	–0.0011	0.0005	0.7033
C14–H11...O11	0.0117	0.0383	0.0085	–0.0074	0.0011	0.8738
C24–I21...N11	0.0171	0.0479	0.0109	–0.0098	0.0011	0.9005
C14–I11...S21 ^b	0.0041	0.0118 ^c	0.0022	–0.0015	0.0007	0.6776
Compound 6						
N2–H22 N...S1	0.0100	0.0305	0.0063	–0.0050	0.0013	0.7877
C1–H1...N1	0.0118	0.0360	0.0075	–0.0059	0.0016	0.7911
C6–H6...I1 ^b	0.0050	0.0147 ^c	0.0029	–0.0022	0.0007	0.7475
C3–I1...N1	0.0126	0.0355	0.0078	–0.0067	0.0011	0.8625
Compound 7						
N2–H2...O1	0.0229	0.0963	0.0208	–0.0175	0.0033	0.8414
C9–H9B...O1	0.0103	0.0348	0.0075	–0.0064	0.0012	0.8445
C6–H6...I1 ^b	0.0052	0.0148 ^c	0.0030	–0.0023	0.0007	0.7691
C6–H6...H9B ^b	0.0020	0.0066 ^c	0.0013	–0.0010	0.0004	0.7315
C3–I1...N1	0.0179	0.0502	0.0115	–0.0104	0.0011	0.9069
Compound 8						
N2–H12 N...N1	0.0113	0.0352	0.0073	–0.0059	0.0015	0.8007
N2–H22 N...N2	0.0140	0.0403	0.0086	–0.0072	0.0014	0.8346
C1–H1...Br1 (1)	0.0093	0.0281	0.0057	–0.0044	0.0013	0.7674
C1–H1...Br1 (2) ^b	0.0046	0.0150 ^c	0.0029	–0.0021	0.0008	0.7170
C4–Br1...S1 (1) ^b	0.0046 ^c	0.0142 ^c	0.0027	–0.0019	0.0008	0.6862
C4–Br1...S1 (2) ^b	0.0013 ^c	0.0040 ^c	0.0007	–0.0004	0.0003	0.5887
C4–Br1...Br1	0.0069	0.0227	0.0045	–0.0033	0.0012	0.7315

^a All unities are given in a.u.

^b These are not considered as hydrogen or halogen interaction.

^c Values which are below the limit.

appropriate parameter to gain a deeper understanding of noncovalent interactions: when $H_b < 0$, the interaction is dominantly covalent, but when $H_b > 0$, the interaction is dominantly electrostatic. The $|V_b|/G_b$ ratio is even more informative: when $|V_b|/G_b > 2$, the interaction is basically covalent, when $|V_b|/G_b < 1$, the interaction is basically electrostatic, but when the ratio is in between, $1 < |V_b|/G_b < 2$, the interaction is intermediate and need to be considered as partially covalent and partially electrostatic. The strong hydrogen and halogen bonds are more covalent in nature, while the weak ones are mainly electrostatic.

From the Table 7, it can be seen that obtained ρ_b values for HBCPs (H stands for hydrogen) are in the range of 0.002–0.023 a.u., whereas the values of $\nabla^2\rho_b$ are all positive, ranging from 0.007 to 0.096 a.u. All of these values are not within the common accepted ranges for H-bonding interactions (ρ_b ranges from 0.002 to 0.040 a.u., $\nabla^2\rho_b$ ranges from 0.020 to 0.150 a.u.) [37–39,58]. Some of the $\nabla^2\rho_b$ values are below the bottom limit and these interactions can not be considered as H-bonds. According to the results obtained, in crystal structure of **3** there are no H-bonding interactions, while in the structures **5**–**8** there are: in **5** four C–H...N/O, in **6** one C–H...N and one N–H...S, in **7** two C/N–H...O and in **8** one C–H...Br and two N–H...N.

For XBCPs (X stands for halogen), ρ_b and $\nabla^2\rho_b$ values are in the range of 0.001–0.018 a.u. and 0.004–0.050 a.u., respectively. Again, all of these values are not within the ranges for halogen bonding interactions (ρ_b ranges from 0.006 to 0.049 a.u., $\nabla^2\rho_b$ ranges from

0.019 to 0.153 a.u.) [59]. Hence, only C–Cl...O in **3**, C–I...O and C–I...N in **5**, C–I...N in **6**, C–I...N in **7**, and C–Br...Br in **8** can be considered as halogen bonds. Moreover, the dihalogen Br...Br bonding shows the amphiphilic character of bromine (σ -hole – equatorial interaction, Fig. 8).

In all cases, BCPs are characterized by small ρ_b values, small and positive $\nabla^2\rho_b$ values, positive H_b , and with ratio $|V_b|/G_b < 1$. All these criteria indicate weak and mainly electrostatic hydrogen and halogen bonding interactions. Furthermore, we can also evaluate their relative strengths since the topological parameters correlate well with the interaction energy. In literature, various interactions were studied and the linear relationships of the interaction energy versus the topological parameters at the BCPs were obtained [39,59–61]. From those correlations, we have concluded that interaction energies of hydrogen and halogen bonds in studied molecules can be classified as weak stabilizing interactions (up to 4 kcal/mol in magnitude) [62]. Among them, N–H...O in **7** is the strongest.

The same conclusions, i.e. hydrogen and halogen bonding interactions are found from X-ray crystal structure analyses (see Table 3). Hence, we can state that the topological analysis of the DFT electron density and its results presented here for geometries taken from the crystal structures may be successfully used to discuss the nature of hydrogen and halogen bonding interactions.

4. Conclusion

X-ray molecular geometries of investigated 6,7-disubstituted 1,3-benzothiazoles, **3** and **5**–**8**, show no discrepancy from common molecular geometry of 1,3-benzothiazole and its derivatives. Calculated molecular structures of compounds **3**, **5**, **6** and **8** are in agreement with the corresponding X-ray ones, while that of **7** is different. Gas phase calculations showed that, due to one intramolecular hydrogen C–H...O bond, **7** is planar, while in the crystal phase two intermolecular N–H...O and C–H...O hydrogen bonds are formed causing its nonplanarity.

The crystal structures of studied compounds are determined mostly by weak and dominantly electrostatic hydrogen and halogen bonding interactions. Hydrogen C–H...O/N/Br, N–H...O/N/S bonds, halogen C–Cl...O, C–I...O/N bonds and Br...Br interactions were found. The π – π interactions participate in additional stabilization of the crystal structures of compounds **3**, **5**, **6** and **8**. The molecular electrostatic potential maps have indicated possible hydrogen and halogen bonding interaction sites in structures **3** and **5** (type I), and **6** and **8** (type II). In compounds of the type I the similar C–Cl...O (**3**) and C–I...O and C–I...N (**5**) halogen bonding patterns are formed, because chlorine and iodine atoms are activated by strong electron withdrawing nitro group in *ortho* position. Such mono-coordinated halogen bonding interactions with only one oxygen atom of the nitro group is commonly observed for chlorine, while known tendency of iodine to form bifurcated contacts is not observed in studied compounds. In compounds of the type II, different bonding patterns of halogens are observed: C–I...N halogen bond in **6**, and C–H...Br hydrogen bond and weak Br...Br dihalogen contact in **8**. The most probable reason for that difference is weaker polar flattening of bromine than iodine atom. Furthermore, halogens in compounds of the type II are not additionally activated by good electron withdrawing group such as nitro group in compounds of the type I.

All of the experimentally observed hydrogen and halogen bonds are confirmed by MEP maps and AIM analysis. Halogen and non-conventional hydrogen bondings have been shown to be a powerful tool in crystal engineering.

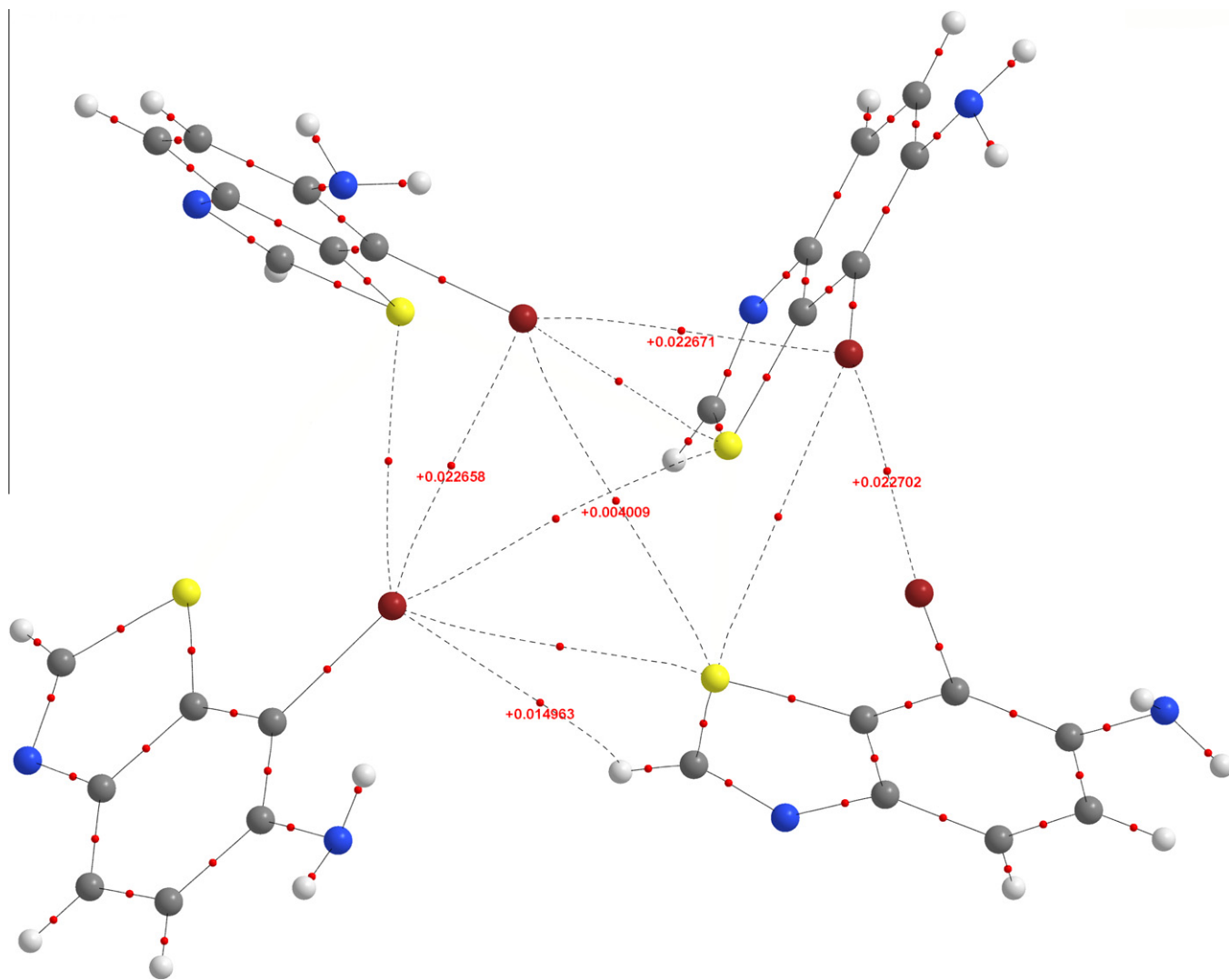


Fig. 8. Molecular graph of tetrameric unit of compound **8**. Small red dots indicate bond critical points (BCPs). Some values of the Laplacian of the electron density are given ($\nabla^2\rho_b$ /a.u.).

Supplementary material

Crystallographic data for the structure in this paper has been deposited at Cambridge Crystallographic Data Centre, 12 Union Road, Cambridge CB2 1EZ, UK (fax: +44 1223 336033; e-mail: deposit@ccdc.cam.ac.uk) and can be obtained on request, free of charge, by quoting the publication citation and the deposition numbers CCDC 740706–740710. Structure factors table is available from the authors.

Acknowledgement

This research was supported by the Ministry of Science, Education and Sports of the Republic of Croatia (Grant Nos. 119-1191342-1339, 119-1193079-1332 and 117-0000000-3283).

References

- [1] C.O. Leong, M. Suggitt, D.J. Swaine, M.C. Bibby, M.F.G. Stevens, T.D. Bradshaw, *Mol. Cancer Ther.* 3 (2004) 1565.
- [2] I. Yildiz-Oren, I. Yalcin, E. Aki-Sener, N. Ucarturk, *Eur. J. Med. Chem.* 39 (2004) 291.
- [3] C. Sheng, J. Zhu, W. Zhang, M. Zhang, H. Ji, Y. Song, H. Xu, J. Yao, Z. Miao, Y. Zhou, J. Zhu, J. Lu, *Eur. J. Med. Chem.* 42 (2007) 477.
- [4] A. Lochart, L. Ye, D.B. Judd, A.T. Merritt, P.N. Lowe, J.L. Morgenstern, G. Hong, A.D. Gee, J. Brown, *J. Biol. Chem.* 280 (2005) 7677.
- [5] Z. Berkovitch-Yellin, L. Leiserowitz, *Acta Cryst.* B40 (1984) 159–165.
- [6] A.V. Afonin, D.-S.D. Toryashinova, E.Yu. Schmidt, *J. Mol. Struct. Theochem.* 680 (2004) 127.
- [7] V.R. Thalladi, A. Gehrke, R. Boese, *New J. Chem.* 24 (2000) 463.
- [8] C. Janiak, T.G. Scharmann, *Polyhedron* 22 (2003) 1123.
- [9] C.N. Sundaresan, S. Dixit, P. Venugopalan, *J. Mol. Struct.* 693 (2004) 205.
- [10] K. Biradha, *CrystEngComm.* 5 (66) (2003) 374.
- [11] M. Mascal, *Chem. Commun.* (1998) 303.
- [12] A. Nangia, *Curr. Opin. Solid State Mater. Sci.* 5 (2001) 115.
- [13] V. Ferretti, L. Pretto, M.A. Tabrizi, P. Gilli, *Acta Cryst.* B62 (2006) 634.
- [14] M. Muthuraman, Y. Le Fur, M. Bagieu-Beucher, R. Masse, J.-F. Nicoud, S. George, A. Nangia, G.R. Desiraju, *J. Solid State Chem.* 152 (2000) 221.
- [15] M. Fourmeigué, *Curr. Opin. Solid State Mater. Sci.* 13 (2009) 36.
- [16] F.H. Allen, J.P.M. Lommerse, V.J. Hoy, J.A.K. Howard, G.R. Desiraju, *Acta Crystallogr.* B53 (1997) 1006.
- [17] L. Racané, V. Tralić-Kulenović, D.W. Boykin, G. Karminski-Zamola, *Molecules* 8 (2003) 342.
- [18] L. Racané, V. Tralić-Kulenović, Z. Mihalić, G. Pavlović, G. Karminski-Zamola, *Tetrahedron* 64 (2008) 11594.
- [19] L. Racané, V. Tralić-Kulenović, R.P. Kitson, G. Karminski-Zamola, *Monatsh. Chem.* 137 (2006) 1571.
- [20] L. Racané, R. Stojković, V. Tralić-Kulenović, G. Karminski-Zamola, *Molecules* 11 (2006) 325.
- [21] D. Matković-Čalogović, Z. Popović, V. Tralić-Kulenović, L. Racané, G. Karminski-Zamola, *Acta Cryst.* C59 (2003) 0190.
- [22] G. Pavlović, L. Racané, H. Čičak, *Dyes Pigments* 83 (3) (2009) 354.
- [23] M. Đaković, H. Čičak, Ž. Soldin, V. Tralić-Kulenović, *J. Mol. Struct.* 938 (2009) 125.

- [24] W.A. Boggust, W.J. Cocker, *J. Chem. Soc.* (1949) 355.
- [25] L. Racač, V. Tralić-Kulenović, G. Pavlović, G. Karminski-Zamola, *Heterocycles* 68 (2006) 1909.
- [26] (a) CrysAlis Software system, Version 1.171.31.8, Xcalibur CCD System, Oxford Diffraction Ltd., 2007, Abingdon, UK;
(b) CrysAlis Software system, Version 1.171.33.27, Xcalibur CCD System, Oxford Diffraction Ltd., 2008, Abingdon, UK.
- [27] G.M. Sheldrick, *Acta Crystallogr. A* 64 (2008) 112.
- [28] L.J. Farrugia, *J. Appl. Crystallogr.* 32 (1999) 837.
- [29] L. Spek, *J. Appl. Crystallogr.* 36 (2003) 7.
- [30] L.J. Farrugia, *J. Appl. Crystallogr.* 30 (1997) 565.
- [31] C.F. Macrae, I.J. Bruno, J.A. Chisholm, P.R. Edgington, P. McCabe, E. Pidcock, L. Rodriguez-Monge, R. Taylor, J. van de Streek, P.A. Wood, *J. Appl. Crystallogr.* 41 (2008) 466.
- [32] M.J. Frisch, G.W. Trucks, H.B. Schlegel, G.E. Scuseria, M.A. Robb, J.R. Cheeseman, et al., *Gaussian 03*, Gaussian Inc., Pittsburgh, PA, USA, 2003.
- [33] R.G. Parr, W. Yang, *Density-functional Theory of Atoms and Molecules*, Oxford Univ. Press, Oxford, 1989.
- [34] EMSL Basis Set Exchange Database, <<https://bse.pnl.gov/bse/portal>>.
- [35] Maestro, version 9.0, Schrödinger, LLC, New York, NY, 2009.
- [36] GaussView 4.1, Gaussian Inc., Pittsburgh, PA, USA, 2006.
- [37] R.F.W. Bader, *Atoms in Molecules: A Quantum Theory*, Oxford Univ. Press, Oxford, 1995.
- [38] P. Popelier, *Atoms in Molecules: An Introduction*, Pearson Education, Harlow, 2000.
- [39] N.J. Martínez Amezaga, S.C. Pamies, N.M. Peruchena, G.L. Sosa, *J. Phys. Chem. A* 114 (2010) 552.
- [40] F. Biegler-König, J. Schönbohm, AIM2000, 2.0 ed., Büro für Innovative Software: Bielefeld, Germany, 2002.
- [41] AIMAll (version 10.03.19), Todd A. Keith, 2010 <aim.tkgristmill.com>.
- [42] H.F. Allen, W.D.S. Motherwell, *Acta Crystallogr. B* 58 (2002) 380.
- [43] I.J. Bruno, J.C. Cole, P.R. Edgington, M. Kesser, C.F. Macrae, P. McCabe, J. Pearson, R. Taylor, *Acta Crystallogr. B* 58 (2002) 389.
- [44] N. Trinajstić, *Tetrahedron Lett.* 12 (1968) 1529.
- [45] F.H. Allen, O. Kennard, D.G. Watson, L. Brammer, A.G. Orpen, R. Taylor, *J. Chem. Soc. Perkin Trans. 2* (1987) S1–S19.
- [46] C. Janiak, *J. Chem. Soc. Dalton Trans.* (2000) 3885.
- [47] C.A. Hunter, J.K.M. Sanders, *J. Am. Chem. Soc.* 112 (1990) 5525.
- [48] C.A. Hunter, *Chem. Soc. Rev.* (1994) 101.
- [49] M.D. Curtis, J. Cao, J.W. Kampf, *J. Am. Chem. Soc.* 126 (2004) 4318.
- [50] F.H. Allen, J.M.P. Lommerse, V.J. Hoy, J.A.K. Howard, G.R. Desiraju, *Acta Crystallogr. B* 53 (1997) 1006.
- [51] J. Bernstein, R.E. Davies, L. Shimoni, N.-L. Chang, *Angew. Chem. Int. Ed. Engl.* 34 (1995) 1555.
- [52] M.C. Etter, *Acc. Chem. Res.* 23 (1990) 120.
- [53] A. Bondi, *J. Phys. Chem.* 68 (1964) 441.
- [54] L. Pauling, *General Chemistry*, third ed., Freeman and Co., San Francisco, 1970.
- [55] F. Blockhuys, C. Peten, C. Van Alsenoy, H.J. Geise, *J. Mol. Struct.* 445 (1998) 187.
- [56] A. Juberta, M.L. Legartob, N.E. Massac, L.L. Tévezd, N.B. Okulikd, *J. Mol. Struct.* 783 (2006) 34.
- [57] E.E. Castellano, O.E. Piro, J.A. Caram, M.V. Mirífico, S.L. Aimone, E.J. Vasini, A. Márquez-Lucero, D. Glossman-Mitnik, *J. Mol. Struct.* 604 (2002) 195.
- [58] M. Domagała, S.J. Grabowski, K. Urbaniak, G. Mlostoń, *J. Phys. Chem. A* 107 (2003) 2730.
- [59] Y.-X. Lu, J.-W. Zou, Y.-H. Wang, Y.-J. Jiang, Q.-S. Yu, *J. Phys. Chem. A* 111 (2007) 10781.
- [60] Y.-X. Lu, J.-W. Zou, Y.-H. Wang, H.-X. Zhang, Q.-S. Yu, Y.-J. Jiang, *J. Mol. Struct. Theochem.* 766 (2006) 119.
- [61] P. Lipkowski, S.J. Grabowski, T.L. Robinson, J. Leszczynski, *J. Phys. Chem. A* 108 (2004) 10865.
- [62] S.J. Grabowski, *Annu. Report Progress Chem., Section C* 102 (2006) 131.